Journal of Applied Electrochemistry (2005) 35:551–560
DOI 10.1007/s10800-005-1519-9

Application of a solid polymer electrolyte reactor to remove nitrate ions from wastewater

H. CHENG*, K. SCOTT and P.A. CHRISTENSEN
*School of Chemical Engineering and Advanced Materials, University of Newcastle upon Tyne, NE1 7RU, England (*author for correspondence, e-mail: hua.cheng@ncl.ac.uk; fax: +44-0191-222-5292)*

Received 21 June 2004; accepted in revised form 24 January 2005

Key words: efficiency, electrolysis, nitrate reduction, PdRh cathode, solid polymer electrolyte reactor

Abstract

The application of a zero gap solid polymer electrolyte (ZGSPE) reactor to deminealise nitrate ions in aqueous wastewater is described. The following performance data for the reduction of a simulated alkaline solution with 16.1 mM nitrate ions under galvanostatic operation were achieved: percentage of nitrate removal up to 100%, rates of nitrate removal up to 0.057 mol cm^{-2} h^{-1}, space–time yields up to 5.4 kg m^{-3} h^{-1}, current efficiencies up to 24.5% and energy consumption between 40.1 and 63.3 kW h kg^{-1}. The beneficial effects of higher temperatures and nitrate ion concentrations and using a suitable electrolyte flow rate on the activity, selectivity and efficiency is reported. $PdRh_{1.5}$/Ti mini-mesh electrode used in the study was stable after a cumulative use of 1000 h.

1. Introduction

Many sources of water, especially in areas of intensive agriculture, contain intolerable levels of nitrate ion [1]. Some industrial sectors, e.g. the nuclear industry, produce large amounts of nitrate wastes [2]. During the treatment of nitrate, by products, such as nitrite and ammonia are also frequently formed which pose greater environmental risks than nitrate [3–5]. The allowable concentrations of such species are very low, e.g. 50 mg NO_3^- dm^{-3} (15 mg NO_3^- dm^{-3} for infants) [1, 6], 0.5 mg NO_2^- dm^{-3} [1, 7] and 0.5 mg NH_3 dm^{-3} [4, 5]. Previous investigation of nitrate reduction has contributed to the understanding of the mechanism and the development of technologies for the removal of nitrate from wastewater [2, 8].

Calcination is unattractive because it requires high temperatures and pressures to form sodium nitrate melts and releases toxic off-gases, e.g. NO_x [9]. Among current technologies for the removal of nitrate ions, ion exchange and reverse osmosis are only considered as pre-treatment methods [8, 10, 11]. Biological treatment of nitrate has problems of contamination, low rate and maintenance [9, 11–13]. Chemical reduction of nitrate using hydrogen or metals has limitations in its effectiveness, stability, safety and cost [14, 15].

Electrochemical reduction is an alternative technology for the removal of nitrates and nitrites from wastes [2, 16–18]. The nitrate ions are reduced according to the following reactions in alkaline media [19, 20]:

$$NO_3^- + H_2O + 2e^- = NO_2^- + 2\ OH^- \quad (1)$$

$$NO_3^- + 3H_2O + 5e^- = \frac{1}{2}N_2 + 6\ OH^- \quad (2)$$

$$NO_3^- + 6H_2O + 8e^- = NH_3 + 9\ OH^- \quad (3)$$

$$NO_2^- + 2H_2O + 3e^- = \frac{1}{2}N_2 + 4\ OH^- \quad (4)$$

$$NO_2^- + 5H_2O + 6e^- = NH_3 + 7\ OH^- \quad (5)$$

The main parasitic reactions are hydrogen and oxygen evolution at the cathode and anode, respectively:

$$2H_2O + 2e^- = H_2 + 2OH^- \quad (6)$$

$$4OH^- = O_2 + 2H_2O + 4e^- \quad (7)$$

The overall reactions to nitrogen and ammonia are [13, 20]:

$$4NaNO_3 + 2H_2O = 2N_2 + 5O_2 + 4NaOH \quad (8)$$

$$NaNO_3 + 2H_2O = NH_3 + 2O_2 + NaOH \quad (9)$$

The cathode material plays an important role in nitrate reduction [9]. Transition metals, e.g. Pt, Pd, Rh, Ru and Ir, and coinage metals, i.e. Cu, Ag and Au, and their binary and ternary combinations have attracted much research [10, 21–23]. Very recently, a patent was filed for the electrolytic removal of nitrate containing water using an Rh coated cathode [24]. Use of packed particle bed Cu, Ni, Fe or Pb electrodes has been used to decrease the concentration of the nitrate in low-level nuclear waste from 1000 to 50 mg dm^{-3} [2, 8].

Electrochemical reduction of nitrate is sensitive to solution composition, and in particularly, the solution pH [10]. For instance, in acid solutions, nitrate reduction occurs on Cu, Cd and Zn, but not on Ni and Pb [25]. Product distribution is highly dependent on the pH of the solution, e.g. ammonia production is favoured at low pH [26]. Both ammonia and hydroxylamine are reported as major products in strong acid (> 5 M H^+) [27].

Product distribution dependence on applied current density was observed; for example, the main gaseous products for nitrate reduction at platinum in concentrated NaOH solutions are nitrogen and ammonia at current densities less than 100 and 460 mA cm^{-2}, respectively [28].

At present, the industrial use of an electrochemical process for nitrate removal is challenged by several factors, e.g. low selectivity to nitrogen, formation of nitrite intermediate, release of ammonia [9] and unsuitable electrodes [10, 17].

The research reported here was carried out to assess a process for electrochemical reduction of nitrate ions to nitrogen, with minimum formation of nitrite and ammonia. A zero gap solid polymer electrolyte (ZGSPE) reactor with a high surface area $PdRh_{1.5}$ cathode was used because it is able to function in various media including pure water. The reactor was used to determine optimum reactor conditions for the nitrate removal with simulated industrial wastewater [8, 10] at laboratory scale. To our knowledge, the use of a solid polymer electrolyte reactor for electrochemical reduction of nitrate has not been previously reported.

2. Experimental details

2.1. *Materials and chemicals*

The following materials and chemicals were used as received: Ti mini-mesh (Ti purity 99.6%, mesh size 1.5 mm, open area 37%, wire diameter 0.2 mm, Goodfellow), $PdCl_2$ (99%, Aldrich), $RhCl_3$ (98%, Aldrich), $NaNO_3$ (99.99%, Aldrich), $NaNO_2$ (99.99%, Aldrich), $NaHCO_3$ (99.7%, Aldrich), NH_4Cl (99.5%, Aldrich), NaOH (99.99%, Aldrich), NaCl (99%, Aldrich), Na_2SO_4 (99%, Aldrich), H_2SO_4 (98%, AnalaR, BDH) and phthalic acid (99.5%, Aldrich).

The simulated wastewater was used as the standard, and consisted of 84.0 g dm^{-3} (1 M) $NaHCO_3$, 0.4 g dm^{-3} (6.8 mM) NaCl, 0.4 g dm^{-3} (2.8 mM) Na_2SO_4 and 1.0 g dm^{-3} (1000 ppm, 16.1 mM) NO_3^- (in the form of $NaNO_3$) [8]. Fresh electrolyte was used for each electrolysis. The nitrate concentration was varied in several experiments. All solutions were prepared using deionised water (ELGASTAT B124 Water Purification Unit, The Elga group, England).

2.2. *Electrode*

A Pd–Rh titanium mini-mesh electrode was prepared by thermal deposition of catalyst. The mesh was abraded with emery paper and rinsed thoroughly with water and then in acetone. Following etching with boiling 37% HCl solution for 5 min, the mesh was put in an oven set at 500 °C for 10 min. After cooling and weighing, the mesh was dipped in ethanol solutions containing the metal salts of concentration 0.2 M and then dried at 500 °C, in air, for 10 min. The dip-heating procedure was repeated until the desired catalyst loading was achieved. The binary catalysts were obtained by repeatedly depositing one catalyst component after another. The deposited mesh was annealed at the deposition temperature (500 °C) for 3 h and then allowed to cool to ambient temperature. The catalyst loading was obtained by weight difference of the mesh before and after deposition, assuming that the most stable oxides were formed during the deposition, i.e. PdO and Rh_2O_3 [19]. Finally, the deposited mesh was post-treated cathodically by electrolysis in 0.25 M H_2SO_4 aqueous solution at a constant current density of 2 mA cm^{-2} for 60 min (Cell voltage varied between 1.8 and 2.1 V). At the start of pre-treatment, the electrolyte became dark in colour and clear again at the end of the electrolysis. The prepared binary electrode was assigned to $PdRh_{1.5}$ according to the atomic ratio of the two metals, based on weight difference of the substrate before and after deposition.

2.3. *Solid polymer electrolyte reactor*

Figure 1 shows the ZGSPE reactor, which consisted of a membrane-electrode assembly (MEA), two stainless steel back-plates (15 cm × 10 cm × 2 cm each), two PTFE channelled plates (15 cm × 10 cm × 2 cm each) with six channels (2 mm in width, 1 mm in depth and 25 mm in length), eight layers of stainless steel mesh (current collectors and turbulence promoters) and two Tiron rubber O-ring seals. The main part of the reactor was a membrane electrode assembly (MEA, 0.6 mm in thickness and 20 cm^2 in active area) obtained by hot pressing the mesh anode and the mesh cathode on either side of the pre-treated Nafion® 117 membranes at 50 kg cm^{-2} and 100 °C for 3 min.

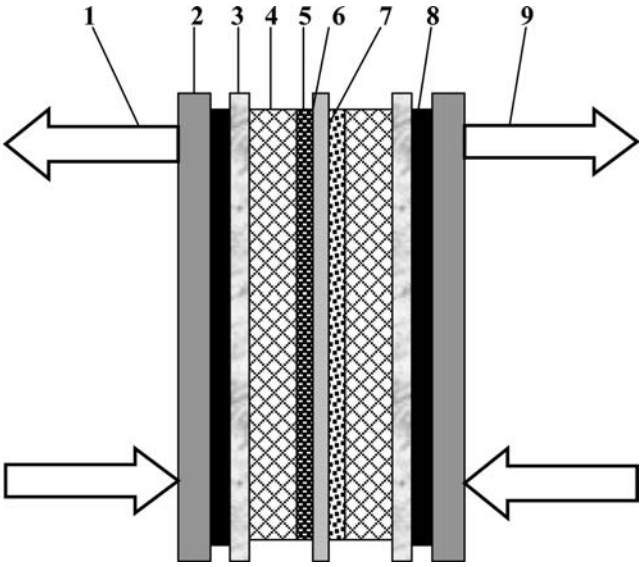

Fig. 1. Zero gap solid polymer electrolyte cell. 1. Catholyte. 2. End plate (stainless steel). 3. Manifold plate (PTFE). 4. Distributor (stainless steel mesh). 5. Cathode ($PdRh_{1.5}$/Ti mini-mesh). 6. Nafion 117 membrane. 7. Anode (Pt/Ti mini-mesh). 8. Seal O-ring (Tiron rubber). 9. Anolyte. The cell dimension is 22 cm × 14 cm × 3 cm.

The reactor was inserted into a circulation loop consisting of peristaltic pumps (Cole-Parmer) and reservoirs (1 dm^3), placed in two heating mantles (Electrothermal® Flask/Funnel, Cole-Parmer) for anolyte and catholyte. After conditioning the MEA at 60 °C and atmospheric pressure with continuous feed of 0.5 M H_2SO_4 solution for 24 h, the reactor was operated in a batch recirculation mode. The off-gases were collected in reservoirs containing 1 M H_2SO_4 aqueous solutions before venting to the atmosphere.

2.4. *Electrochemical measurements*

Electrode polarisation curves were obtained in a three-electrode H-cell divided by a Nafion® 117 membrane using cyclic voltammetry and steady-state measurements using a ministat potentiostat, a PCI-100 computer interface and an EC Prog v3 Software (Sycopel Scientific Limited). The working electrode was a $PdRh_{1.5}$/Ti mini-mesh (0.75 mg Pd + 1.09 mg Rh cm^{-2}, 1.2 cm^2). A commercial saturated calomel electrode (SCE, Russell) and a platinum mesh (20 cm^2, Goodfellow) were used as reference and counter electrodes, respectively. All potentials are quoted against the SCE reference electrode. All of the solutions studied were thoroughly degassed using oxygen free nitrogen (BOC Ltd). The working electrode was cycled between 0.4 and −1.2 V at a scan rate of 50 mV s^{-1} three times before collecting stable polarisation data.

2.5. *Batch electrolysis*

Batch electrolysis was performed in the ZGSPE reactor controlled at a constant current density (1, 5, 10 or 20 mA cm^{-2}) using a FARNELL LS60-5 power supply for periods up to 150 h. The catholyte was mixed using magnetic stirrer. Samples were taken at regular intervals and were analysed for NO_3^-, NO_2^- and NH_3 concentrations and for pH. The final data included ammonia detected by absorption in a 50 cm^3 1 M H_2SO_4 solution.

2.6. *Product analysis*

Concentrations of nitrate and nitrite were determined by high-performance liquid chromatography (HPLC). The HPLC system, supplied by DIONEX, consisted of a P 580 Pump and a Softron 2000 UVD 170S/340S UV/vis detector with an Whatman Partisil 5 ODS-3 column (5 μm particle size and 25 × 0.46 cm, Alltech Associates, Inc.). The wavelengths used in the HPLC measurements were determined using UV–vis spectroscopy (UV-160A UV-Visible Recording Spectrophotometer, SHIMADZU, Japan). Normally, the UV detector was set to 320 nm for nitrate detection and 360 nm for nitrite detection. The mobile phase was a 4 mM phthalic acid aqueous solution with a flow rate of 1.0 cm^3 min^{-1}. The peaks for nitrate ions (retention time 3.15 min) and nitrite ions (retention time 3.90 min) were characterised by using standard solutions. Quantification of the product distribution during the electrolysis was accomplished using calibration curves prepared from authentic samples (Aldrich). The calibrations for the standard solutions (1.0×10^{-5} to 0.2 mol dm^{-3}) using a sample volume of 20 μl were carried out three times for each compound and the data were averaged. The detection limits of this method was 1 ppm for nitrate ions and 0.3 ppm for nitrite ions under the experimental conditions.

Ammonia was analysed with an Orion Model 95-12 Ammonia (NH_3) Gas Sensing Combination Electrode connected to an Orion digital Ion/pH meter (Corning Model 135, Corning Glass Works or Orion model 920A, Orion Research, Inc.). Calibration curves were obtained using standard solutions of 5×10^{-5} to 0.15 mol dm^{-3} NH_4Cl, prepared using the standard ammonium chloride solution (Orion 951006) and the ionic strength adjustor solution (Orion 951211) at the operating temperature. The calibrations were carried out before and after each experiment. Test samples were prepared for analysis by putting 1–5 cm^3 samples into a 25 cm^3 standard flask and diluting to the mark with ionic strength adjuster solution (Orion 951211).

The amounts of nitrogenous gas (mainly nitrogen in alkaline solution [4]) were obtained from the amounts of nitrite and ammonia from the amount of reduced nitrate [4, 15]. No evidence of other possible products, such as hydroxylamine (NH_2OH) and hydrazine (N_2H_4), formed in the electrolysed solutions was found using standard chemical analysis methods [29].

2.7. *Parameter definitions*

Reactor performance indicators used were normalised percentage of nitrate removal (χ), space–time yield (γ) and average rate of nitrate removal (β); selectivity using

yields of nitrogen (ξN_2), ammonia (ξNH_3) and nitrite (ξNO_2), current efficiency (ϕ_i or ϕ) and energy consumption (ψ_i or ψ_R), defined as [30, 31]:

$$\chi = \frac{C_0 - C_t}{C_0} \times 100\% \tag{12}$$

$$\gamma_i = \frac{3600 \times \alpha \times j \times \phi_i \times M_{FW}}{n_i \times F} \tag{13a}$$

$$\gamma = \Sigma\left(\frac{C_i}{C_0 - C_t} \times \gamma_i\right) \tag{13b}$$

$$\beta = \frac{(C_0 - C_t) \times V}{t \times A} \tag{14}$$

$$\xi_i = \frac{C_i}{C_0 - C_t} \times 100\% \tag{15}$$

$$\phi_i = \frac{m_i \times n_i \times F}{q} \tag{16a}$$

$$\phi = \Sigma\phi_i \tag{16b}$$

$$\psi_i = \frac{n_i \times F \times E_{Cell}}{\phi_i \times M_{FW}} \tag{17a}$$

$$\psi_R = \Sigma\left(\frac{C_i}{C_0 - C_t} \times \psi_i\right) \tag{17b}$$

where C_0 and C_t are concentrations of nitrate (mol dm^{-3}) at start and at an electrolysis time t (h), respectively, C_i is the concentration of nitrogen, ammonia or nitrite (mol dm^{-3}) at t (h), α is a specific area (m^{-1}), defined as a ratio of the electrode area to the volume of the batch of solution undergoing treatment, j is the current density (A m^{-2}), n_i is the number of electrons in the reaction forming i (i = nitrogen, ammonia, nitrite, etc.), F is the Faraday constant (96485 C mol^{-1}), M_{FW} is the molar mass of nitrate ions (kg mol^{-1}), V is the volume of the batch of solution undergoing treatment (dm^3), A is the geometric area of cathode (m^2), m_i is the quantity of the formed species i (mole) and q is the total electrical charge (C) and E_{Cell} is the cell voltage. ψ_i and ψ_R are individual and total energies consumed, respectively.

Considering the fact that different percentages of initial $NaNO_3$ were converting to intermediates according to Equations 1–3 in alkaline solutions, a weighting parameter (equal to $\frac{C_i}{C_0 - C_t}$) was introduced in Equations 13b and 17b to calculate the contribution to the total value of a parameter from each reaction.

3. Results and discussion

3.1. *Voltammetric characteristics*

Figure 2 shows a cyclic voltammogram, using the normalised current density, obtained on a $PdRh_{1.5}$/Ti mini-mesh electrode in a simulated solution (1.0 mol dm^{-3} $NaHCO_3$ + 6.8 mM dm^{-3} NaCl + 2.8 mM dm^{-3} Na_2SO_4 solution) with or without 0.1 M $NaNO_3$ [8] at ambient temperature. A cathodic plateau was observed between −0.70 and −0.80 V vs SCE in the blank solution due to reduction of hydrogen-containing species in solution. The current increased rapidly after −0.80 V, which is attributed to hydrogen evolution, as evidenced by gas bubbles evolving from the electrode surface. A distinct anodic current peak corresponding to oxidation of hydrogen species was observed at −0.41 V.

The addition of 0.1 M NO_3^- led to an increase in reduction currents after −0.48 V, indicating that nitrate reduction occurred simultaneously with hydrogen evolution. The data clearly show that, in the presence of NO_3^-, there is a significant change in the oxidation peak, i.e. a decrease in the peak current density and a negative shift of the peak potential from −0.41 to −0.69 V, which was accompanied by an increase in the reduction current due to nitrate reduction (Figure 2). These shifts imply a change of the electrode surface due to nitrate reduction [27].

Overall, the results of voltammetric measurements demonstrated a strong involvement of hydrogen species

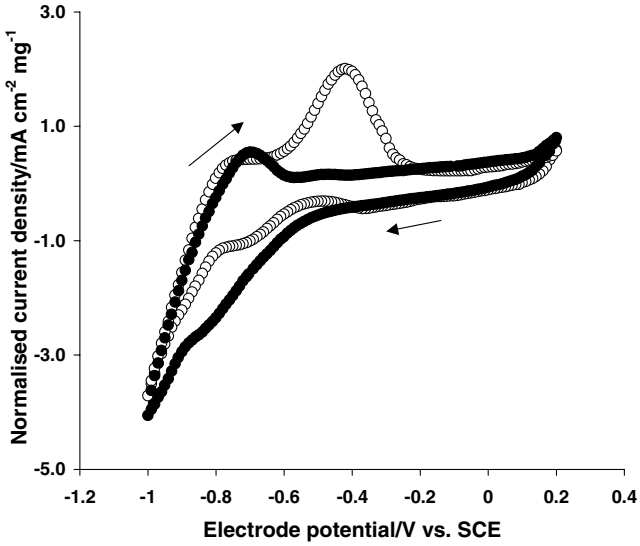

Fig. 2. Cyclic voltammetric curves on the $PdRh_{1.5}$/Ti mini-mesh electrode in the alkaline solution with and without nitrate ions. Cell: H-cell divided by a Nafion® 117 membrane. Cathode: $PdRh_{1.5}$/Ti mini-mesh (0.75 mg Pd + 1.09 mg Rh cm^{-2}, 1.3 cm^2); Anode: Pt mesh (20 cm^2). Catholyte: 1.0 M $NaHCO_3$ + 6.8 mM. NaCl + 2.8 mM Na_2SO_4 solution with (●) or without (○) 0.1 M $NaNO_3$ (100 cm^3). Anolyte: 1.0 M $NaHCO_3$ solution (100 cm^3). Scan rate: 5 mV s^{-1}. Temperature: 17.5 ± 1.0 °C. The arrows indicate scan directions.

in nitrate ion reduction [17]. The presence of adsorbed nitrate ions and hydrogen species at the cathode surface during the nitrate reduction has been confirmed [15, 32]. Hydrogen adatoms compete with nitrogen species for active sites and thus hinder nitrate reduction or, successively, the released hydrogen atoms hydrogenated the intermediates formed [2–5].

Apart from intrinsic activity of Rh and Pd for nitrate reduction, the effectiveness of the $PdRh_{1.5}$/Ti mini-mesh electrode for nitrate reduction can be attributed to synergetic effects, resulting from local electronic modification and active site distribution induced by the mixing of different catalysts [33, 34]. The metal–metal combination modified the electronic environment and changed structure parameters such as bonding distance and bonding energy, reaction mechanism, etc., compared to single catalyst. Consequently, new reaction units were formed to provide the catalytically active surface and to determine the participation of different types of intermediates associated with ensembles of different size [35]. Such an effect has been demonstrated with binary and ternary catalysts showing better catalytic activity, than the single catalysts, in terms of the reduction of nitrates and prevention of formation of ammonium [36, 37].

3.2. *Bulk electrolysis – influence of current density*

The effect of applied current density on current efficiency in batch electrolysis, with the ZGSPE reactor using a $PdRh_{1.5}$/Ti mini-mesh electrode, during the reduction of the simulated nitrate solution, is shown in Figure 3. A current density of 1 mA cm^{-2} gave the highest current efficiencies for nitrate reduction to nitrogen, which fell from 95.0% to 52.4%. It is shown in Figure 3 that the current efficiency decreased with increasing current density. A current density of 5 mA cm^{-2}, led to lower current efficiencies, i.e. falling from 22.5 to 10.8%. At higher current densities, the current efficiencies were even lower, e.g. 7.0–9.2% at 10 mA cm^{-2} and 3.5–4.3% at 20 mA cm^{-2}. The decrease in current efficiencies was probably due to higher hydrogen gas generation in the structure of the electrode. In effect a partial current density of approximately 1 mA cm^{-2} is associated with nitrate reduction to nitrogen at the start of each electrolysis. A current density of 5 mA cm^{-2} was used in later nitrate reduction as it still exhibited a relatively high current efficiency, together with the higher partial current density for nitrate reduction to nitrogen at the end of the electrolysis, i.e. $\varphi \times j \approx 0.7$, c.f. 0.5 at 1 mA cm^{-2}.

During the electrolysis, a substantial change in average cell voltage was observed, e.g. after 24 h electrolysis, 1.6, 2.9, 5.0 and 7.4 V for current densities of 1, 5, 10 and 20 mA cm^{-2}, respectively (Table 1). The cell voltage and higher current efficiencies translated into a substantial energy savings for the operation of the reactor at low current densities, i.e. 16.0 and 230.7 kW h kg^{-1} at 1 and 20 mA cm^{-2}, respectively (Table 1).

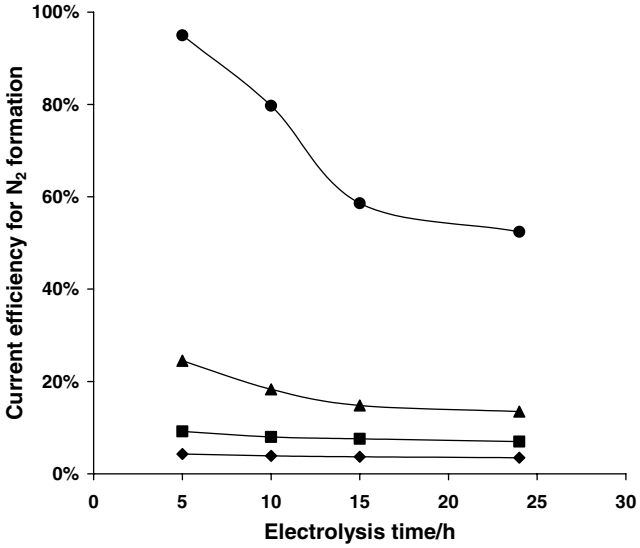

Fig. 3. Effect of controlled current density on current efficiency for the nitrogen formation during the electrochemical reduction of nitrate in a solid polymer electrolyte reactor. Current density: ● 1 mA cm^{-2}; ▲ 5 mA cm^{-2}; ■ 10 mA cm^{-2}; ◆ 20 mA cm^{-2}. Reactor: Zero gap solid polymer electrolyte reactor divided by a Nafion® 117 membrane. Cathode: $PdRh_{1.5}$/Ti mini-mesh (0.75 mg Pd + 1.09 mg Rh cm^{-2}, 20 cm^2). Anode: Pt/Ti mini-mesh (2.03 mg Pt cm^{-2}, 20 cm^2). Catholyte: 16.1 mM $NaNO_3$ in 1.0 M $NaHCO_3$ + 6.8 mM NaCl + 2.8 mM Na_2SO_4 solution (170 cm^3). Anolyte: 1.0 M $NaHCO_3$ solution (170 cm^3). Flow rate of electrolytes: 50 cm^3 min^{-1}. Temperature: 18.5 ± 1.5 °C.

More data on the effect of current density on nitrate reduction in the ZGSPE reactor are shown in Table 1. Generally, increasing current density led to increases in the percentage of nitrate removal, space–time yield and average reaction rate. However, the effect was more pronounced from 1 to 10 mA cm^{-2}; only small changes were observed at higher current densities (Table 1). The amounts of by-products formed during nitrate reduction also varied with applied current density, e.g. ammonia yield increased from 1.1 to 7.5% when the current density was increased from 1 to 5 mA cm^{-2}, suggesting that the formation of ammonia was more favourable at higher current densities.

It is interesting to note the variation of solution pH with current density during electrolysis. The pH of the treated solutions gradually became more alkaline while the anolytes became more acidic during electrolysis, mainly due to the side reactions (Equations 6 and 7). The maximum pH of 11.6, after 24 h electrolysis was observed at 10 mA cm^{-2}. The lower pH at 20 mA cm^{-2} was caused by greater proton transfer through the Nafion® membrane. The different final pH values at different current densities suggests that the production of H^+ did not match the production of OH^- ion. More alkaline media decreased nitrite and ammonia formation and suppressed hydrogen evolution during nitrate reduction [4].

Table 1. Effect of controlled current density on nitrate reduction in the ZGSPE reactor[a]

	Current density (mA cm^{-2})			
	1	5	10	20
χ (%)	57.7	73.9	94.9	100
γ (kg m^{-3} h^{-1})	3.2	4.0	5.2	5.4
β (mol cm^{-2} h^{-1})	0.033	0.042	0.054	0.057
ξ_{NO_2} (%)	0	0	0	0
ξ_{NH_3} (%)	1.1	2.4	2.9	7.5
ξ_{N_2} (%)	98.9	97.6	97.1	92.5
ϕ (%)[b]	52.4	13.5	7.0	3.5
ψ (k W h kg^{-1})[b]	16.0	74.0	151.8	230.7
Catholyte pH[c]	8.68	9.61	11.59	9.96
Anolyte pH[d]	7.20	5.12	1.85	1.04
E_{Cell}	1.6	2.2	5.0	7.4

[a]The conditions are as in Figure 3 and all data were collected at 24 h.
[b]Data for nitrogen formation.
[c]The initial pH was 7.65.
[d]The initial pH was 7.45.

During electrolysis, hydrogen evolution took place simultaneously in the potential region of nitrate reduction. So nitrate was reduced on the electrode while generated hydrogen adatoms took part in nitrate reduction. The hydrogen adatoms compete with nitrogen species for the active sites and thus hinder nitrate reduction and/or the released hydrogen atoms hydrogenate the intermediates formed and the absorbed hydrogen atom react with nitrate [2–5, 15]. In addition, hydrogen evolution occurred in the solution and, overall processes determine the activity, selectivity and efficiency of the process.

3.3. *Bulk electrolysis – influence of nitrate concentration and temperature*

Figure 4 shows the average rates of nitrate removal during constant current electrolysis in the ZGSPE reactor using a $PdRh_{1.5}$/Ti mini-mesh cathode at 5 mA cm^{-2} in the simulated solution with different concentrations of nitrate. When the concentration of $NaNO_3$ was lower than 1 mM, the rate of nitrate removal was low, i.e. between 0.00027 and 0.0037 mol cm^{-2} h^{-1}. With an increase in concentration of $NaNO_3$, the rate increased significantly, i.e. around 0.06 and 0.10 mol cm^{-2} h^{-1} in 16.1 and 100 mM solutions, respectively. A higher concentration increased mass transfer of nitrate to the electrode and thus increased the rate of nitrate removal.

Table 2 shows that nitrate concentration had a significant effect on space–time yield, i.e. at 24 h, values of 0.03, 0.3, 4.7 and 9.8 kg m^{-3} h^{-1} in 0.1, 1.0, 16.1 and 100 mM nitrate solutions, respectively. These changes were caused mainly by changes in the rate of nitrate removal.

The nitrate concentration also affected the current efficiency, e.g. at 24 h, 0.09, 0.87, 13.0 and 29.2% for the nitrogen formation in 0.1, 1.0, 16.1 and 100 mM nitrate solutions, respectively (Table 2). Current efficiency also decreased with the electrolysis time, since nitrate concentration decreased and hydrogen evolution gradually increased with time.

An increase in nitrate concentration significantly reduced energy consumption, e.g. after 24 h electrolysis, 46.4×10^2, 927, 34.5 and 37.1 kW h kg^{-1} (based on the nitrate reduction) in 0.1, 1.0, 16.1 and 100 mM nitrate solutions, respectively (Table 2). The higher energy consumption in the dilute solutions was a direct consequence of the lower current efficiencies and increased cell voltage, e.g. 0.3 V higher in 0.1 mM nitrate, compared to 100 mM (Table 2). The selectivity of nitrate reduction was approximately constant over the range of nitrate concentration investigated (Table 2). For each solution, reaction rate, selectivity and

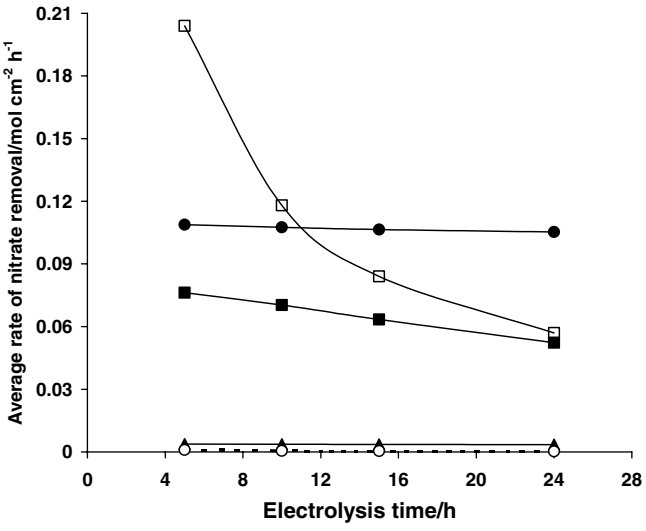

Fig. 4. Effect of nitrate concentration and temperature on rate of nitrate removal during the electrochemical reduction of nitrate in a solid polymer electrolyte reactor. Concentration of nitrate: ● 100 mM; ■ 16.1 mM; □ 16.1 mM, 80 °C; ▲ 1 mM; ○; 0.1 mM. Flow rate of electrolytes: 50 ml min^{-1}. Other conditions as in Figure 3.

Table 2. Effect of concentration of nitrate and temperature on nitrate reduction[a]

	Concentration (mM)				
	0.1	1.0	16.1	16.1 (80 °C)	100
χ (%)[b]	100	100	91.7	100	35.7
γ (kg m^{-3} h^{-1})	0.03	0.3	4.7	5.2	9.8
β (mol cm^{-2} h^{-1})	0.00027	0.0035	0.052	0.057	0.105
ξ_{NO_2} (%)	0	0	0	0	0
ξ_{NH_3} (%)	5.6	6.3	6.8	16.0	7.5
ξ_{N_2} (%)	94.4	93.7	93.2	84.0	92.5
ϕ (%)[c]	0.09	0.87	13.0	12.6	29.2
ψ (k W h kg^{-1})[b]	46.4×10^2	927	34.5	21.0	37.1
E_{Cell} (V)	2.3	2.3	2.1	1.1	2.0

[a]The conditions are as in Figure 4 and all data were collected at 24 h.
[b]Non-normalised data based on the nitrate reduction.

efficiency of the nitrate reduction decreased shortly after the start of electrolysis.

Figure 4 shows the influence of the reaction temperature (18.5–80 °C) on nitrate reduction in the ZGSPE reactor. Increasing temperature favoured ammonia formation and reduced nitrogen formation (Table 2), as previously reported [2]. A reason for this was due to different pH change of the catholyte at different temperature during the electrolysis, e.g. at 24 h, the catholyte pH changed from 7.65 to 9.61 to 10.34 at 18.5 ± 1.5 °C and 80 °C, respectively. The pH change was a natural result of the various reactions of nitrate reduction (Equations 1–3). In basic solutions, increasing pH could suppress hydrogen evolution and increase ammonia formation [32]. Consequently, the current efficiency for nitrogen formation decreased slightly when the temperature was increased from 18.5 to 80 °C (Table 2).

In general, increasing temperature could affect the reduction rate of nitrate in several ways, for example, by increasing the rate of diffusion and the strength of the adsorption.

The percentage of nitrate removal, space–time yield and rate of nitrate removal increased with increasing temperature. For example, the rate of nitrate removal at 80 °C was three times higher than that at 18.5 °C at the initial stage of electrolysis (Figure 3) and only increased by 0.005 mol cm^{-2} h^{-1} at 24 h, as the nitrate concentration was much lower at 24 h. As the temperature increased, the energy consumption decreased, e.g. at 24 h, the values were 34.5 and 21.0 kW h kg^{-1} at 18.5 and 80 °C, respectively (Table 2). The effect was mainly due to the decrease in the cell voltage, i.e. 2.1 and 1.1 V at 18.5 and 80 °C, respectively (Table 2).

3.4. *Bulk electrolysis – influence of flow rate*

The influence of electrolyte flow rate on the percentage of nitrate removal is shown in Figure 5. The percentages of nitrate removed were nearly identical at flow rates of 50 and 100 cm^3 min^{-1} (ca. 92%) and were higher than at the lower flow rate of 15 cm^3 min^{-1} (74%). At low flow rates, e.g. 15 cm^3 min^{-1}, there was lower mass transfer rate, as observed previously during nitrate reduction in a catalytic membrane reactor [4].

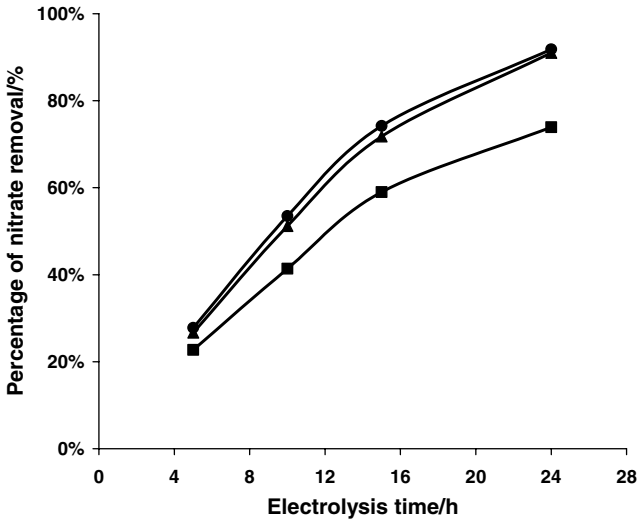

Fig. 5. Effect of flow rate on percentage of nitrate removal. Flow rate: ● 50 cm^3 min^{-1}; ■ 15 cm^3 min^{-1}; ▲ 100 cm^3 min^{-1}. Other conditions as in Figure 3.

A variation in selectivity of nitrate reduction with flow rate was observed in this study, e.g. at 24 h, the nitrogen yields were 88.9, 94.0 and 98.8% at 15, 50 and 100 cm^3 min^{-1}, respectively and the ammonia yield decreased from 10.1% at 15 cm^3 min^{-1} to 1.2% at 100 cm^3 min^{-1} (Table 3). Higher flow rates benefited nitrogen formation while ammonia formation was suppressed, which can be partially attributed to differences in mass transfer at different flow rates.

3.5. *Bulk electrolysis – long duration experiment*

Experiments of 150 h were carried out to assess the effectiveness and stability of the ZGSPE reactor, particularly for the cathode. Figures 6–8 show the average data from two 150 h electrolyses of 100 mM $NaNO_3$ + 1.0 M $NaHCO_3$ + 6.8 mM NaCl + 2.8 mM Na_2SO_4 solution (170 cm^3), using the $PdRh_{1.5}$/Ti

Table 3. Effect of flow rate of electrolyte on nitrate reduction in the ZGSPE reactor[a]

	Flow rate (cm^3 min^{-1})		
	15	50	100
χ (%)	73.9	91.7	91.0
γ (kg m^{-3} h^{-1})	4.0	4.7	5.1
β (mol cm^{-2} h^{-1})	0.042	0.052	0.052
ξ_{NO_2} (%)	0	0	0
ξ_{NH_3} (%)	10.1	6.0	1.2
ξ_{N_2} (%)	88.9	94.0	98.8
ϕ (%)[b]	10.0	13.0	13.5
ψ (k W h kg^{-1})[b]	40.0	37.7	31.7
E_{Cell} (V)	2.1	2.1	2.0

[a]The conditions are as in Figure 6 and all data were collected at 24 h.
[b]Data for nitrogen formation.

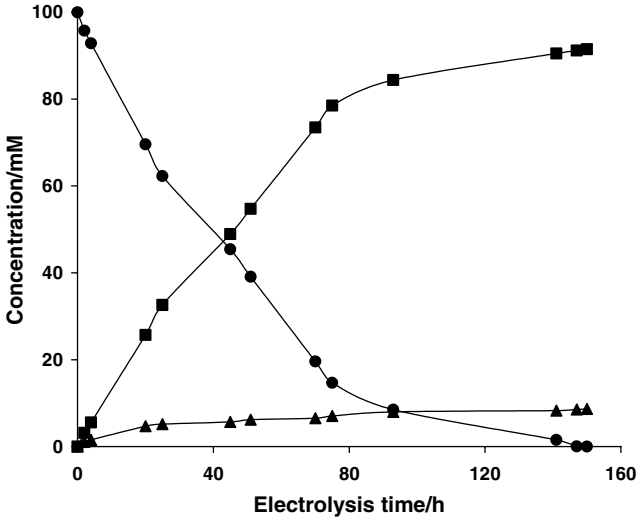

Fig. 6. Long-term evaluation of the nitrate reduction in a solid polymer electrolyte reactor – concentration change. ● NO_3^-; ■ N_2; ▲ NH_3. Catholyte: 100 mM $NaNO_3$ in 1.0 M $NaHCO_3$ + 0.4 g dm^{-3} NaCl + 0.4 g dm^{-3} Na_2SO_4 solution (170 cm^3). Anolyte: pure water (170 cm^3). Flow rate of electrolytes: 50 ml min^{-1}. Other conditions as in Figure 3.

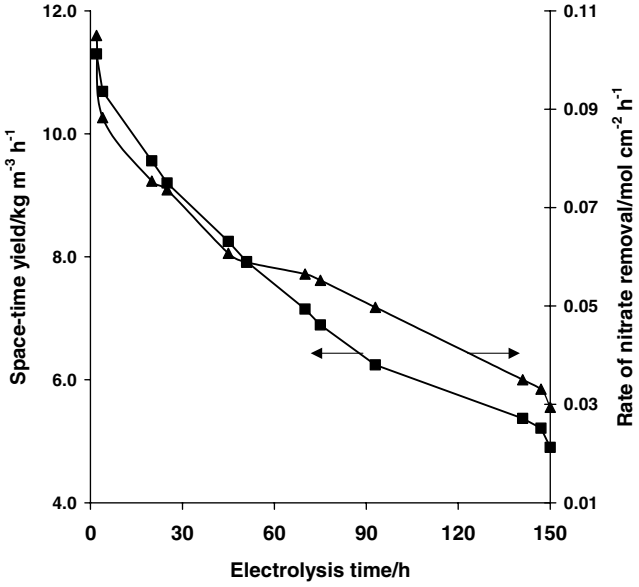

Fig. 7. Long-term evaluation of the nitrate reduction in a solid polymer electrolyte reactor – space–time yield (γ) and removal rate (β). ■ γ; ▲ β. Conditions as in Figure 6.

mini-mesh cathode at a current density of 5 mA cm^{-2}. Conversion of nitrate steadily increased and finally, reached 100% with concomitant formation of nitrogen and ammonia (Figure 6). The amount of nitrogen reached high values within 80 h, after which the amounts of nitrogen concentrations levelled off. The concentration of ammonia increased gradually and finally reached a value of 8.7 mM (Figure 6). The initial increase in nitrogen and ammonia can be explained by the relatively high reaction rates of Equations 2 and 3 (nitrate to nitrogen and to ammonia). The levelling off in nitrogen after 80 h of electrolysis was attributed to the decrease in concentration of nitrate in the treated solution and the consequentially gradual decrease in the nitrogen production rate. No nitrite ions were detected during the electrolysis due to the high selectivity of the $PdRh_{1.5}$/Ti mini-mesh cathode for nitrate reduction to ammonia and nitrogen. Other possible intermediates, e.g. NH_2OH, were also not detected and, possibly, because their reduction in alkaline solutions was faster than in acidic solutions [38]. Thus, only the overall reactions providing stable products were considered here. Other possible intermediate steps were not considered in this work.

Both the space–time yield and rate of nitrate removal during the long duration experiment decreased with electrolysis time, as shown in Figure 7, which were due to a decrease in nitrate concentration. Current efficiency and energy consumption were in the ranges 15–54% and 25–85 kW h kg^{-1}, respectively (Figure 7). The decrease in the current density was mainly due to the decrease in reduction rate, which was a consequence of a decrease in nitrate concentration. Increased cell voltage (2.6–3.1 V after 150 h) resulted in an increase in the energy consumption.

The high activity, high selectivity and high efficiency observed during the long duration experiments were

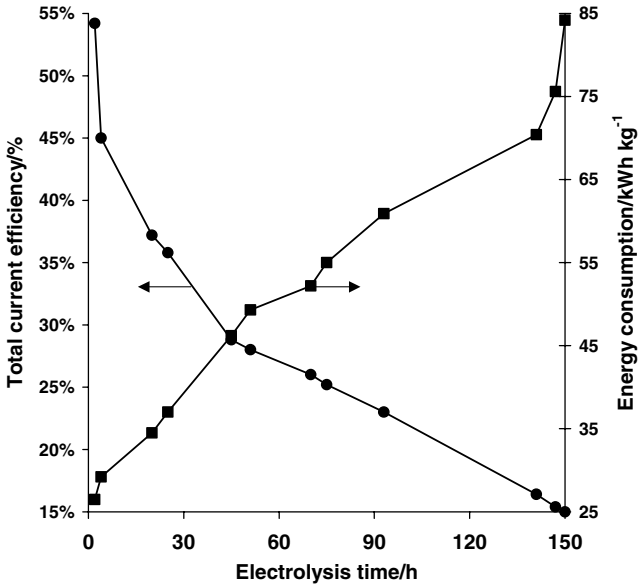

Fig. 8. Long-term evaluation of the nitrate reduction in a solid polymer electrolyte reactor – current efficiency (ϕ) and energy consumption (ψ). ● ϕ; ■ ψ. Conditions as in Figure 6.

mainly attributed to the activity of the $PdRh_{1.5}$/Ti mini-mesh electrode. After a cumulative use of 1000 h (including two 150 h repeated experiments), the $PdRh_{1.5}$/Ti mini-mesh electrode was stable and had no obvious loss in catalytic activity (similar results were still obtained when the cathode was used to repeat several runs). The potential use of the electrode in large-scale or long-term electrolyses without the necessity to regenerate the electrode surface, has been demonstrated to a significant extent.

3.6. *Comparison between ZGSPE reactor and H-cell*

Table 4 compares the reduction of nitrate in the ZGSPE reactor and in an H-cell. Higher values of the percentage of nitrate removal, space–time yields, rate of nitrate removal and current efficiency were achieved in the H-cell, compared to the ZGSPE reactor (Table 4), mainly due to difference in the cathode surface areas used in the two cells and the contact of the cathode with the Nafion® membrane in the ZGSPE. In the ZGSPE reactor, part of the cathode surface area was blocked by the current collector and the membrane; both sides of the cathode surface in the H-cell could fully contact the catholyte. Improvement in design of the ZGSPE reactor structure should provide a further improvement in the reactor performance. The selectivity achieved in the two types of cell was similar, but lower energy consumption was observed in the ZGSPE reactor compared to the H-cell. A substantial voltage drop of 1.1 V at a current density of 5 mA cm^{-2} was observed, which compensated for a lower current efficiency.

It was noted that the reduction of nitrate in pure water and in the simulated solution using the ZGSPE reactor achieved similar performance data, as shown in Table 4. This has an important implication, i.e. no restrictions in medium and/or in nitrate concentration for the reduction of nitrate wastewater in the ZGSPE reactor, which offers an attractive technology to treat various wastes.

High ammonia concentration was observed after the long duration electrolysis. The problem could be addressed via paired electrolysis (simultaneous reduction of nitrate and oxidation of ammonia) and this related work will be reported elsewhere.

The data reported are similar or better than other reported results, e.g. reduction of the nitrate concentration from 600 to 50 mg dm^{-3} with a current efficiency of 22% and ammonia as a main product, during reduction of nitrate in $NaHCO_3$ solutions at a copper plate cathode in an undivided flow-through reactor [13]. Higher current efficiency, e.g. 40%, and very low energy consumption, e.g. 0.05 kW h kg^{-1}, have been reported [2, 8, 39]. These results indicate the potential use of three-dimensional materials in ZGSPE reactor to enhance mass transfer and increase process efficiency.

Table 4. Comparison of the ZGSPE reactor with the H-cell for nitrate reduction[a]

	Cell					
	ZGSPE reactor		ZGSPE reactor (H_2O)		H-cell	
	Value	Normalised	Value	Normalised	Value	Normalised
χ (%)	56.8	30.8	54.6	29.7	70.4	38.3
γ (kg m^{-3} h^{-1})	8.3	4.5	8.4	4.6	8.6	4.7
β (mol cm^{-2} h^{-1})	0.11	0.06	0.10	0.056	0.13	0.07
ξ_{NO_2} (%)	0	0	0	0	0	0
ξ_{NH_3} (%)	12.7	6.9	10.4	5.7	13.2	7.2
ξ_{N_2} (%)	87.3	47.4	89.6	48.7	86.8	47.2
ϕ (%)[b]	24.6	13.4	24.3	13.2	30.3	16.5
ψ (k W h kg^{-1})[b]	43.2		46.1		50.6	
E_{Cell} (V)	2.9		2.8		4.0	

[a]All data were collected at 45 h. The conditions for the ZGSPE reactor are as in Figure 6. The conditions for the H-cell – Cathode: $PdRh_{1.5}$/Ti mini-mesh cathode (0.75 mg Pd + 1.09 mg Rh cm^{-2}, 9 cm^2); Anode: Pt mesh (20 cm^2). Catholyte: 0.1 M $NaNO_3$ in 1.0 M $NaHCO_3$ solution (75 cm^3). Anolyte: 1.0 M $NaHCO_3$ solution (75 cm^3). Controlled current density: 5 mA cm^{-2}. Temperature: 15.5 ± 1.5 °C.
[b]Data for nitrogen formation.

4. Conclusions

Treatment of nitrate wastes using a ZGSPE reactor has been demonstrated. At high current densities, e.g. 20 mA cm^{-2}, high percentages of nitrate removal up to 100%, high rate of nitrate removal up to 0.057 mol cm^{-2} h^{-1} and high space–time yields up to 5.4 kg m^{-3} h^{-1} were achieved. The current efficiency was, however, low, i.e. in a range of 3.5–4.3%, and the energy consumption was in the range of 170–231 kW h kg^{-1} for the reduction of a simulating solution containing 16.1 mM nitrate. The reduction of the same nitrate solution at low current densities, e.g. 5 mA cm^{-2}, improved current efficiency to a range of 13.5–24.5% and thus reduced the energy consumption to a range of 40.1–63.3 kW h kg^{-1}. The low current density also increased the nitrogen yield and decreased the ammonia yield.

The rate of nitrate removal, the space–time yield and the current efficiency increased significantly and the energy consumption decreased significantly with increasing nitrate concentration. Percentage of nitrate removal, space–time yield and rate of nitrate removal increased with increasing temperature. Increasing temperature favoured ammonia formation and reduced nitrogen formation. Use of a high electrolyte flow rate of 50–100 cm^3 min^{-1} led to a high percentage of nitrate removal. Use of higher flow rates increased nitrogen formation and suppressed ammonia formation.

The effectiveness and stability of the ZGSPE reactor was evaluated in long duration experiments of 150 h. The complete removal of 100 mM nitrate was achieved with nitrogen as the main product. The $PdRh_{1.5}$/Ti mini-mesh electrode provided stable performance over a cumulative use of 1000 h without obvious loss of catalytic activity.

The reduction of nitrate in pure water was carried out in the ZGSPE reactor, which demonstrated that the technology could be used to treat nitrate wastes with different levels of nitrate ions.

Acknowledgements

The authors thank the United Kingdom Engineering and Physical Sciences Research Council (EPSRC) for funding. The work was performed in research facilities provided through an EPSRC/HEFCE Joint Infrastructure Fund award (No. JIF4NESCEQ).

References

1. N.F. Gray, *'Drinking Water Quality: Problems and Solutions'* (John Wiley and Sons Ltd., Chichester, 1994), pp. 21.
2. J.O'M. Bockris and J. Kim, *J. Appl. Electrochem.* **27** (1997) 623.
3. M. Badea, A. Amine, G. Palleschi, D. Moscone, G. Volpe and Curulli A., *J. Electronal. Chem.* **509** (2001) 66.
4. K. Lüdtke, K.-V. Peinemann, V. Kasche and R.-D. Behling, *J. Membrane Sci.* **151** (1998) 3.
5. http://www.ohd.hr.state.or.us/dwp/docs/fact/ammonia.pdf.
6. EEC Council Recommendations (1987).
7. EEC Council Directive 98/83/EC (1998).
8. M. Paidar, K. Bouzek and H. Bergman, *Chem. Eng. J.* **85** (2002) 99.
9. http://www.lanl.gov/projects/nitrate/Other.htm.
10. K. Bouzek, M. Paidar, A. Sadilkova and H. Bergmann, *J. Appl. Electrochem.* **31** (2001) 1185.
11. C.-P. Huang, H.-W. Wang and P.-C. Chiu, *Wat. Res.* **32** (1998) 2257.
12. A. Kapoor and T. Viraraghavan, *J. Environ. Eng.* **4** (1997) 371.
13. M. Paidar, I. Rousar and K. Bouzek, *J. Appl. Electrochem.* **29** (1999) 611.
14. K.M. Hiscock, J.W. Lloyd and D.N. Lemer, *Wat. Res.* **25** (1991) 1099.
15. C.L. Clement, N.A. Nado, A. Katty, M. Bernard, A. Deneuville, C. Comninellis and A. Fujishima, *Diamond Related Mater.* **12** (2003) 606.
16. J.O'M. Bockris and J. Kim, *J. Electrochem. Soc.* **143** (1996) 3801.
17. J.D. Genders, D. Hartsough and D.I. Hobbs, *J. Appl. Electrochem.* **26** (1996) 1.
18. E.E. Kalu, R.E. White and D.I. Hobbs, *J. Electrochm. Soc.* **143** (1996) 3094.
19. D.R. Lide and H.P.R. Frederikse (eds), *CRC Handbook of Chemistry and Physics*, 78th ed., (CRC Press, New York, 1997) Section 8.
20. W.J. Plieth, *in* A.J. Bard (Ed.), *'Encyclopaedia of Electrochemistry of the Elements'*, (Marcel Dekker, 1978), Vol. VIII, Chapter 5.
21. G.E. Dima, A.C.A. Vooys de and M.T.M. Koper, *J. Electroanal. Chem.* **554–555** (2003) 15.
22. M.T. Groot de and M.T.M. Koper, *J. Electroanal. Chem.* **562** (2004) 81.
23. J.F.E. Gootzen, P. G.J.M. Peeters, J.M.B. Dukers, L. Lefferts, W. Visscher and J.A.R. Veen van, *J. Electroanal. Chem.* **434** (1997) 171.
24. IONEX LTD., British Patent 2,348,209 (2001).
25. B.R. Scharifker, J. Mostany and A. Serruya, *Electrochem. Commun.* **2** (2000) 448.
26. S.-H. Cheng and Y.O. Su, *Inorg. Chem.* **33** (1994) 5847.
27. D. Pletcher and Z. Poorabedi, *Electrochim. Acta* **24** (1979) 1253.
28. H.-L. Li, D.H. Robertson and J.A. Chambers, *J. Electrochem. Soc.* **135** (1988) 1154.
29. A.I. Vogel, *'Vogel's Textbook of Quantitative Chemical Analysis'*, 5th ed., Revised by G.H. Joffery, J. Bassett, J. Mendham and R.C. Denney, Longman Scientific & Technical (1997) p. 408 or pp. 402–403 for determination of hydroxylamine or hadrazine, respectively.
30. F. Goodridge and K. Scott, *'Electrochemical Process Engineering'* (Plenum Press, New York, 1995), pp. 15–191.
31. D. Pletcher and F.C. Walsh, *'Industrial Electrochemistry'*, 2nd ed., (Chapman and Hall, New York, 1990) Chapter 2.
32. T. Ohmori, M.S. El-Deab and M. Osawa, *J. Electroanal. Chem.* **470** (1999) 46.
33. D.W. McKee, A.J. Scarpellino Jr., I.F. Danzig and M.S. Pak, *J. Electrochem. Soc.* **116** (1969) 562.
34. N. Alonso-Vante. 'Catalysis and Electrocatalysis at Nonoparticle Surfaces', *in* A. Wieskowki, E.R. Sauliroua and C. Vayeras (eds), Catalysis and Electrocatalysis at Nanoparticle Surfaces, (Marcel Dekker, New York, 2003).
35. L. Guczi, *J. Mol. Catal.* **25** (1984) 13.
36. O.M. Ilinitch, L.V. Nosova, V.V. Gorodetskii, V.P. Ivanov, S.N. Trukhan, E.N. Gribov, S.V. Bogdanov and F.P. Cuperus, *J. Mol. Catal. A: Chemical* **158** (2000) 237.
37. S.R. Gavagnin, F. Pinna, E. Modaferri, S. Perathoner, G. Centi, M. Marella and M. Tomaselli, *Catal. Today* **55** (2002) 139.
38. A.C.A. Vooys de, M.T.M. Koper, R.A. Santenvan and J.A.R. Veenvan, *Electrochim. Acta* **46** (2001) 923.
39. A.S. Koparal and U.B. Ogutveren, *J. Hazardous Mater.* **89** (2002) 83.